Article

Chiroptical Effects in the Second Harmonic Signal of Collagens I and IV

Ana-Maria Pena, Thierry Boulesteix, Thibault Dartigalongue, and Marie-Claire Schanne-Klein

J. Am. Chem. Soc., **2005**, 127 (29), 10314-10322• DOI: 10.1021/ja0520969 • Publication Date (Web): 02 July 2005

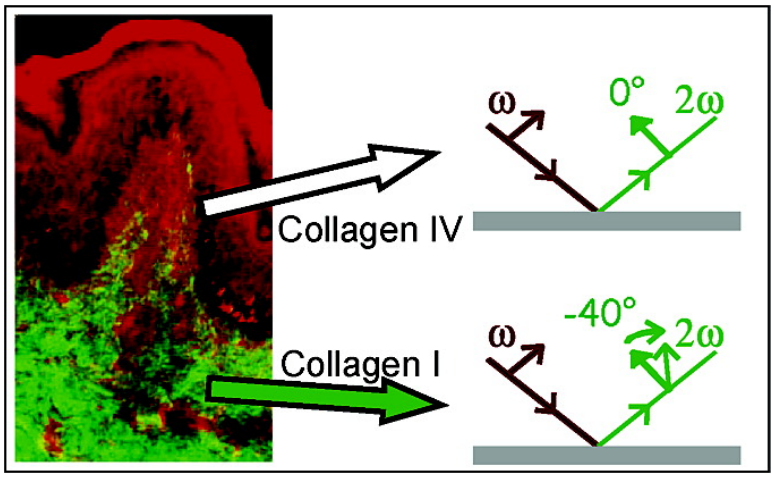

More About This Article

Additional resources and features associated with this article are available within the HTML version:

- Supporting Information
- Links to the 3 articles that cite this article, as of the time of this article download
- Access to high resolution figures
- Links to articles and content related to this article
- Copyright permission to reproduce figures and/or text from this article

View the Full Text HTML

J|A|C|S
ARTICLES
Published on Web 07/02/2005

Chiroptical Effects in the Second Harmonic Signal of Collagens I and IV

Ana-Maria Pena, Thierry Boulesteix, Thibault Dartigalongue, and Marie-Claire Schanne-Klein*

Contribution from the Laboratory for Optics and Biosciences, CNRS/INSERM, Ecole polytechnique, 91128 Palaiseau, France

Received April 1, 2005; E-mail: marie-claire.schanne-klein@polytechnique.fr

Abstract: We performed polarization-resolved surface second harmonic generation (SHG) experiments on thin films of collagen I and IV molecules, as well as conventional CD measurements. We found that collagen IV presents little CD and no SHG optical activity, whereas collagen I exhibits large chiroptical effects involving both one-electron and excitonic coupling mechanisms. We estimated that these chiral components enhance the SHG signal from fibrillar collagen in biological tissues by typically a factor of 2. By comparing the distinct behaviors of collagens I and IV in SHG microscopy and in surface SHG experiments, we concluded that SHG microscopy is a sensitive probe of the micrometer-scale structural organization of collagen in biological tissues.

1. Introduction

Collagens are the most abundant proteins in the extracellular matrix, and they play a central role in the formation of fibrillar and microfibrillar networks, basement membranes, as well as other structures of connective tissue.[1] Second harmonic generation (SHG) by fibrillar collagen in a rat tail tendon was first reported in the 1980s by Freund et al.[2] More recently, multiphoton microscopy based on endogenous sources of nonlinear signals emerged as a valuable tool to study live unstained tissue, and SHG microscopy was applied to the observation of connective tissue.[3−7] Several studies were performed to characterize the polarization properties as well as the amplitude and structural variations of the SHG from fibrillar collagen.[8−11] It was reported that nonfibrillar collagens produce no SHG.[6,12] It was proposed that the large SHG signal from collagen was due to the dense and highly ordered structure of the collagen fibers, and that this signal may be further enhanced by the chirality of collagen.[5,13]

The characteristic feature of a collagen molecule is indeed its long, triple helical structure in which three polypeptide chains, called α *chains*, are wrapped around one another in a ropelike right-handed superhelix. Thus far, 27 genetically distinct collagen types have been described, each of them having different structures, functions, and distribution in tissues.[14] The helical domain of the α-chains presents one glycine residue in every third position of the polypeptide chain, resulting in a $(Gly-X-Y)_n$ repeated structure. The number of repeats, *n*, varies between collagen types. In the case of fibrillar collagens, the helical domain of the α-chains is continuous over a length of typically 1000 amino acids, while the nonfibrillar collagens commonly contain imperfections in the helical sequence leading to interruptions by noncollagenous domains. The helical domain of the α-chains assembles in a way that all glycine residues occupy a central position in the triple helix, whereas the others amino acids X and Y have their bulky side chains in the outer positions. Being the smallest amino acid (having only one hydrogen atom as a side chain), glycine allows the three helical α-chains to tightly pack together to form the final collagen superhelix, known as the procollagen molecule.

The most abundant family of collagens with more than 90% of the total collagen consists of the fibril-forming collagens: mainly collagen I, which is a $[\alpha1(I)_2]\alpha2(I)$ heterotrimer, and collagens II, III, V, and XI. They are found in a wide variety of tissues such as bone, tendon, skin, ligament, cornea, and internal organs. For those types, the procollagen molecules are secreted into the extracellular matrix and then cleaved to collagen molecules that finally self-assemble into fibrils. The fibrils are 10 to 300 nm in diameter and up to several hundred

(1) Bateman, J. F.; Lamandé, S. R.; Ramshaw, J. A. M. In *Extracellular matrix, Vol. 2: Molecular components and interactions*; Comper, W. D., Ed.; Harwood Academic Publisher: Amsterdam, 1996; Chapter 2.
(2) Freund, I.; Deutsch, M.; Sprecher, A. *Biophys. J.* **1986**, *50*, 693−712.
(3) Guo, Y.; Ho, P. P.; Savage, H.; Harris, D.; Sacks, P.; Schantz, S.; Liu, F.; Zhadin, N.; Alfano, R. R. *Opt. Lett.* **1997**, *22*, 1323−1325.
(4) Stoller, P.; Reiser, K. M.; Celliers, P. M.; Rubenchik, A. M. *Biophys. J.* **2002**, *82*, 3330−3342.
(5) Campagnola, P. J.; Millard, A. C.; Terasaki, M.; Hoppe, P. E.; Malone, C. J.; Mohler, W. A. *Biophys. J.* **2002**, *82*, 493−508.
(6) Zipfel, W. R.; Williams, R. M.; Christie, R.; Nikitin, A. Y.; Hyman, B. T.; Webb, W. W. *Proc. Natl. Acad. Sci. U.S.A.* **2003**, *100*, 7075−7080.
(7) König, K.; Riemann, I. *J. Biomed. Opt.* **2003**, *8*, 432−439.
(8) Kim, B. M.; Eichler, J.; Reiser, K. M.; Rubenchik, A. M.; Da Silva, L. B. *Lasers Surg. Med.* **2000**, *27*, 329−335.
(9) Theodossiou, T.; Rapti, G.; Hovhannisyan, V.; Georgiou, E.; Politopoulos, K.; Yova, D. *Lasers Med. Sci.* **2002**, *17*, 34−41.
(10) Stoller, P.; Celliers, P. M.; Reiser, K. M.; Rubenchik, A. M. *Appl. Opt.* **2003**, *42*, 5209−5219.
(11) Williams, R. M.; Zipfel, W. R.; Webb, W. W. *Biophys. J.* **2005**, *88*, 1377−1386.
(12) Brown, E.; McKee, T.; diTomaso, E.; Pluen, A.; Seed, B.; Boucher, Y.; Jain, R. K. *Nat. Med.* **2003**, *9*, 796−800.
(13) Zoumi, A.; Yeh, A.; Tromberg, B. J. *Proc. Natl. Acad. Sci. U.S.A.* **2002**, *99*, 11014−11019.
(14) Gelse, K.; Pöschl, E.; Aigner, T. *Adv. Drug Delivery Rev.* **2003**, *55*, 1531−1546.

10.1021/ja0520969 CCC: $30.25

micrometers long, depending on the tissues. The fibrils can be oriented differently depending on tissue type.[15] In tendon, collagen I fibrils align parallel to each other and form bundles or fibers, whereas in the skin the orientation is more random and interlaced fibrils form a complex network. A fiber can be 1−20 μm in diameter, with a mean diameter between 0.5 and 3 μm.

Other collagens do not form fibrils, such as collagen IV, which is found mainly in basement membranes. Collagen IV molecule is composed of three domains: the central triple helix containing numerous short interruptions to the Gly−X−Y sequence, the N-terminal domain, and the C-terminal globular domain. Individual collagen IV molecules assemble to form a two-dimensional network in the matrix.[16] Collagen IV exists predominantly as an $[\alpha1(IV)_2]\alpha2(IV)$ heterotrimer.

In this article, we study the role of chirality in the SHG from collagens I and IV, using polarization-resolved experiments. For that purpose, we need to separate the effects of macroscopic orientation from the effects of the noncentrosymmetry at the molecular scale. Therefore, we studied isolated collagen triple helices arranged in a somehow isotropic way. In these conditions, it is suitable to perform surface SHG from a thin isotropic film of collagen triple helices.[17] Practically, this experimental setup has a geometry similar to that of SHG microscopy from dyes inserted in membranes, where the centrosymmetry was shown to be a critical parameter.[18−20] More generally, chiroptical effects in surface SHG have been extensively studied for the last 10 years, and polarization-resolved surface SHG has proven to be highly sensitive to molecular chirality.[21−32]

In the following, we present a comprehensive study of the chiroptical properties of different types of collagen, including polarization-resolved surface SHG experiments and conventional circular dichroism (CD) spectroscopy. To fully characterize our samples, we also performed absorption, one-photon-excited fluorescence (1PEF), and two-photon-excited fluorescence (2PEF) measurements, as well as transmission electron microscope (TEM) images. We compared fibril-forming collagen I and nonfibrillar collagen IV because they do not present the same behavior in SHG microscopy as illustrated by combined 2PEF and SHG images of epithelial tissue. We discuss our results in the theoretical framework of SHG optical activity, considering both the electric and magnetic dipolar contributions. Finally, we derive a typical order of magnitude for the chiral contribution to the SHG signal in collagens I and IV.

2. Materials and Methods

2.1. Multiphoton Laser Scanning Microscopy. Combined 2PEF and SHG imaging was performed using a custom-built laser scanning microscope incorporating a femtosecond titanium−sapphire laser (Mira, Coherent), galvanometer mirrors (GSI Lumonics), and photon-counting photomultiplier modules (Electron Tubes).[33] Detection channels were implemented in both the reflected and transmitted directions to allow for simultaneous detection of 2PEF and SHG signals using appropriate filters.[19] We used a 20×, 0.95-NA objective lens (Olympus) to combine a large field of view and a high spatial resolution. In the experiments reported here, the objective back aperture was underfilled, resulting in 0.8 effective excitation NA. Thin histological cuts were illuminated with typically 4 mW average power at 814 nm, which resulted in no visible laser-induced morphological alterations.

2.2. Thin Film Preparation. We used collagen I powder extracted from rat tails with acetic acid (Sigma-Aldrich, product number C7661). This type of extraction preserves the integrity of the collagen molecule and enables the formation of fibrils under physiological conditions. The powder was dissolved in 0.1 N acetic acid to obtain a working concentration of 1 mg/mL. Collagen IV powder was extracted from Engelbreth−Holm−Swarm mouse sarcoma in the presence of reducing agent (Sigma-Aldrich, product number C0543). Collagen IV solution was reconstituted to a concentration of 1.5 mg/mL in 0.25% acetic acid.

For each type of collagen, a few microliters of the prepared solution were deposited on optically flat fused silica substrates, suitable for surface SHG experiments. Before deposition, the substrates were carefully washed and underwent a hydrophilic treatment with a Piranha solution ($^2/_3$ H_2SO_4 and $^1/_3$ H_2O_2) to ease the attachment of collagen on the substrate. After 1 min, the samples were washed with ultrapure water to remove the unattached collagen and then dried at room temperature. This deposition method was repeated two or three times to obtain a thin layer.

2.3. Absorption, Fluorescence, CD Spectra, and TEM Images. Absorption measurements were performed using a CARY500 Varian spectrophotometer, and 1PEF measurements were taken using an F-4500 Hitachi spectrofluorimeter. Thin film absorption spectra were recorded using a bare substrate on the reference channel.

2PEF spectra were recorded using femtosecond titanium−sapphire laser (Tsunami, Spectra-Physics), a 20×, 0.4 NA IR objective (Olympus), a spectrometer (H10, Jobin Yvon), and a photomultiplier tube (H5783P, Hamamatsu). This "two-photon spectrofluorimeter" was calibrated with a fluorescein solution (pH = 11, concentration 5.5 μmol/L).[34]

CD spectra were recorded using a CD6 Jobin-Yvon CD Spectrometer, in 100-μm-long quartz (fused silica) cells.

We performed TEM experiments on collagen I in the acetic acid solution only and then we added NaCl (30 mg of NaCl and 0.75 mg of collagen I in 1 mL of acetic acid). Solution drops of each sample type were deposited on carbon-coated electron microscope grids and stained with uranyl acetate 1%. Controlled preparations were done without any staining to check for any eventual effect of the stain on aggregation. The grids were then observed and images recorded on a Philips CM12 transmission electron microscope operating at 120 kV.

2.4. Polarization-Resolved SHG Setup. Surface SHG experiments were performed in a reflection geometry as previously described[17,27]

(15) Hulmes, D. J. S. *J. Struct. Biol.* **2002**, *137*, 2−10.
(16) Yurchenco, P. D.; Schittny, J. C. *FASEB J.* **1990**, *4*, 1577−1590.
(17) Shen, Y. R. *Annu. Rev. Phys. Chem.* **1989**, *40*, 327−350.
(18) Campagnola, P. J.; Mei, M.-d.; Lewis, A.; Loew, L. M. *Biophys. J.* **1999**, *77*, 3341−3349.
(19) Moreaux, L.; Sandre, O.; Blanchard-Desce, M.; Mertz, J. *Opt. Lett.* **2000**, *25*, 320−322.
(20) Moreaux, L.; Sandre, O.; Charpak, S.; Blanchard-Desce, M.; Mertz, J. *Biophys. J.* **2001**, *80*, 1568−1574.
(21) Petralli-Mallow, T. P.; Wong, T. M.; Byers, J. D.; Yee, H. I.; Hicks, J. M. *J. Phys. Chem.* **1993**, *97*, 1383−1388.
(22) Byers, J. D.; Yee, H. I.; Hicks, J. M. *J. Chem. Phys.* **1994**, *101*, 6233−6241.
(23) Kauranen, M.; Van Elshocht, S.; Maki, J. J.; Persoons, A. *J. Chem. Phys.* **1994**, *101*, 8193−8199.
(24) Verbiest, T.; Kauranen, M.; Persoons, A.; Ikonen, M.; Kurkela, J.; Lemmetyinen, H. *J. Am. Chem. Soc.* **1994**, *116*, 9203−9205.
(25) Maki, J. J.; Kauranen, M.; Persoons, A. *Phys. Rev. B* **1995**, *51*, 1425−1434.
(26) Hecht, L.; Barron, L. D. *Mol. Phys.* **1996**, *89*, 61−80.
(27) Schanne-Klein, M.-C.; Hache, F.; Roy, A.; Flytzanis, C.; Payrastre, C. *J. Chem. Phys.* **1998**, *108*, 9436−9443.
(28) Hache, F.; Mesnil, H.; Schanne-Klein, M.-C. *J. Chem. Phys.* **2001**, *115*, 6707−6715.
(29) Schanne-Klein, M.-C.; Boulesteix, T.; Hache, F.; Alexandre, M.; Lemercier, G.; Andraud, C. *Chem. Phys. Lett.* **2002**, *362*, 103−108.
(30) Hache, F.; Boulesteix, T.; Schanne-Klein, M.-C.; Alexandre, M.; Lemercier, G.; Andraud, C. *J. Phys. Chem. B* **2003**, *107*, 5261−5266.
(31) Schanne-Klein, M. C.; Mesnil, H.; Boulesteix, T.; Hache, F. *Recent Res. Dev. Chem. Phys.* **2003**, *4*, 487−517.
(32) Kriech, M. A.; Conboy, J. C. *J. Am. Chem. Soc.* **2005**, *127*, 2834−2835.
(33) Boulesteix, T.; Beaurepaire, E.; Sauviat, M.-P.; Schanne-Klein, M. C. *Opt. Lett.* **2004**, *29*, 2031−2033.
(34) Xu, C.; Webb, W. W. *J. Opt. Soc. Am. B* **1996**, *13*, 481−491.

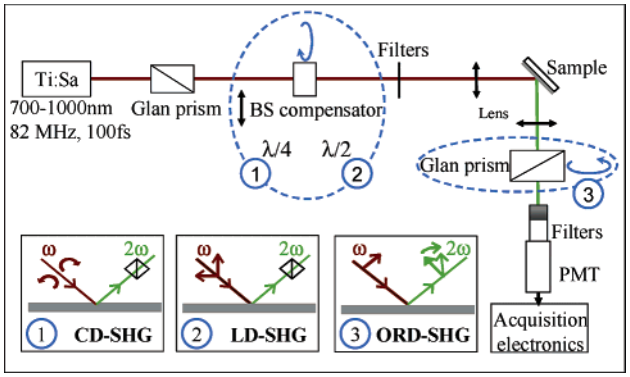

Figure 1. Polarization-resolved surface SHG experimental setup. The insets show the three kinds of experiments relevant to probe the molecular chirality, as described in the Theoretical Background section. The BS compensator is set as a quarter-wave plate for the CD-SHG experiments or as a half-wave plate for the LD-SHG ones. BS: Babinet−Soleil, PMT: photomultiplier tube, Ti:Sa: titanium−sapphire laser.

(see Figure 1). Excitation was provided either by an 82 MHz titanium−sapphire femtosecond laser (Tsunami, Spectra-Physics), tunable in the 700−1000 nm range, or by a 1 kHz custom-built two-stage noncollinear optical parametric amplifier (NOPA) visible source. The laser beam was focused with a 50 mm focal length lens on the sample, resulting in a 45 μm diameter spot when using the titanium−sapphire laser tuned at 800 nm, at an incidence angle of $\alpha = 45°$. After appropriate spectral and spatial filtering, the SHG signal was detected by a photon-counting photomultiplier (PM) module and a counter/timer module (P25PC and CT2, Electron Tubes). The signal was integrated over 500 ms and averaged over 20 measurements. Measured PM dark noise in the absence of laser beam (typically 80 photons/s) was subtracted from the sample signal to remove any insignificant background.

As in usual linear chiroptical measurements, SHG optical activity was measured through its polarization effects. The polarization of the incoming laser beam was adjusted using a Babinet−Soleil compensator, set as a half- or quarter-wave plate, and the polarization of the harmonic beam was analyzed through a rotating Glan prism. This polarization-resolved experiment was also used to determine the relative phase of the various contributions to the SHG signal. For that purpose, we rotated azimuthally the Babinet−Soleil compensator to continuously vary the phase difference between the s and p polarization components at the fundamental frequency.[29,35,36]

3. Theoretical Background

3.1. Physical Origin of Nonlinear Chiroptical Effects. SHG is a coherent second-order nonlinear effect and is forbidden in centrosymmetric media, in particular in liquids of achiral molecules. However, reflection geometry may be used to break the centrosymmetry, and surface SHG has been extensively used to study thin films of molecules since the first experiments by Shen and co-workers.[17] Chiral molecules lack inversion symmetry, and sum frequency generation in a liquid of chiral molecules was reported recently.[37] When considering surface SHG from an isotropic layer of chiral molecules, the centrosymmetry is then broken by both the surface and the molecular chirality. It is then possible to observe two types of nonlinear chiroptical effects in surface SHG, corresponding to different types of molecular chirality.[28,31]

First, as SHG is an even-order nonlinear optical technique, it is possible to evidence chiroptical contributions even in the electric dipolar approximation. These local contributions, first observed by Hicks and co-workers,[21] are typical for molecules exhibiting a chiral arrangement of achiral chromophores, as for example in the case of excitonic coupling.[28,38] The rotational strength of the molecule results from the coupling of two noncoplanar electric dipoles, and model calculations show that electric dipolar contributions are expected to dominate the nonlinear optical activity.[28] Experiments performed with an acridine-substituted Tröger base have shown a good agreement with a model based on coupled anharmonic oscillators.[30]

Second, chiroptical effects may involve electric quadrupolar or magnetic dipolar contributions. These nonlocal contributions[39] are responsible for the usual optical activity in linear optics. In SHG experiments, such contributions were first observed by Persoons and co-workers.[23] They are typical for molecules exhibiting a chiral center,[28,40] where the transitions are electric and magnetic dipolar allowed. Chiral molecules involving an electromagnetic coupling mechanism presumably exhibit the same behavior.

In the general case, nonlinear chiroptical effects are a mix of local and nonlocal contributions. In the following sections, we will consider both contributions and derive the relevant polarization-resolved SHG experiments that proved to be appropriate to study molecular chirality.

3.2. Polarization-Resolved SHG Formalism. The theory of SHG from chiral molecules deposited on a substrate has been extensively treated elsewhere.[22,23,25,27] Here we briefly describe the formalism used to discuss our experimental results and explain the sensitivity of this technique to molecular chirality. The thin collagen layer is described in terms of surface second-order susceptibilities. In addition to the usual electric dipolar susceptibility χ^{eee}, we introduce effective "magnetic" second-order susceptibilities χ^{eem} and χ^{mee}. They account for both electric quadrupolar and magnetic dipolar contributions, which are merged together to simplify the calculations, since it was shown that they cannot be separated experimentally.[23,28] χ^{eem} accounts for those contributions at the fundamental frequency, and χ^{mee} at the harmonic frequency.

We consider the special case of an isotropic surface; in that manner, we exclude all orientation effects and ensure that the measured polarization effects are due to the molecular chirality. This assumption is necessary to evidence unambiguously SHG optical activity[41] and is verified experimentally for our collagen thin films (see next section). It results in a reduced number of nonvanishing independent components in the susceptibility tensors. Some components vanish unless the molecular surface is chiral, that is, has a C_∞ symmetry and are called "chiral" components, whereas the other nonvanishing components correspond to a $C_{\infty v}$ symmetry of the surface and are called "achiral" components. Considering an $x-y$ surface normal to the z direction, the only nonvanishing components are χ^{eee}_{zzz},$\chi^{eee}_{zxx} = \chi^{eee}_{zyy}$,$\chi^{eee}_{xxz} = \chi^{eee}_{yyz} = \chi^{eee}_{xzx} = \chi^{eee}_{yzy}$ (achiral) and $\chi^{eee}_{xyz} = \chi^{eee}_{xzy} = -\chi^{eee}_{yxz} = -\chi^{eee}_{yzx}$ (chiral) for the electric susceptibility and χ^{mee}_{zzz},

(35) Geiger, F.; Stolle, R.; Marowsky, G.; Palenberg, M.; Felderhof, B. U. *Appl. Phys. B* **1995**, *61*, 135−141.
(36) Maki, J. J.; Verbiest, T.; Kauranen, M.; Elshocht, S. V.; Persoons, A. *J. Chem. Phys.* **1996**, *105*, 767−772.
(37) Belkin, M. A.; Han, S. H.; Wei, X.; Shen, Y. R. *Phys. Rev. Lett.* **2001**, *87*, 113001−113003.
(38) Eliel, E.; Wilen, S. H. *Stereochemistry of organic compounds*; Wiley: New York, 1994.
(39) Akhmanov, S. A.; Zharikov, V. I. *JETP Lett.* **1967**, *6*, 137−140.
(40) Schanne-Klein, M.-C.; Hache, F.; Brotin, T.; Andraud, C.; Collet, A. *Chem. Phys. Lett.* **2001**, *338*, 159−166.
(41) Verbiest, T.; Kauranen, M.; Rompaey, Y. V.; Persoons, A. *Phys. Rev. Lett.* **1996**, *77*, 1456−1460.

$\chi^{mee}_{zxx} = \chi^{mee}_{zyy}, \chi^{mee}_{xxz} = \chi^{mee}_{yyz} = \chi^{mee}_{xzx} = \chi^{mee}_{yzy}, \chi^{eem}_{zzz}, \chi^{eem}_{zxx} = \chi^{eem}_{zyy}, \chi^{eem}_{xzx} = \chi^{eem}_{yzy}, \chi^{eem}_{xxz} = \chi^{eem}_{yyz}$ (chiral) and $\chi^{mee}_{xyz} = \chi^{mee}_{xzy} = -\chi^{mee}_{yxz} = -\chi^{mee}_{yzx}$, $\chi^{eem}_{xyz} = -\chi^{eem}_{yxz}, \chi^{eem}_{xzy} = -\chi^{eem}_{yzx}, \chi^{eem}_{zxy} = -\chi^{eem}_{zyx}$ (achiral) for the magnetic susceptibilities.

The reflected harmonic field $E(2\omega)$ is a function of the tensorial components of all these susceptibilities and of the fundamental electric field $E(\omega)$ impinging on the surface with incidence angle θ. Because the relevant experimental parameters are the electric field polarization components E_s (perpendicular to the plane of incidence) and E_p (parallel to the plane of incidence), it is convenient to use the (k,s,p) referential, where k is the wave vector, and to introduce the f, g, and h parameters:

$$E_{s,p}(2\omega) \propto f_{s,p}E_p^2(\omega) + g_{s,p}E_s^2(\omega) + h_{s,p}E_p(\omega)E_s(\omega) \quad (1)$$

Detailed expressions of these parameters are given in the Supporting Information. They all mix together local and nonlocal contributions, except g_s, which comprises nonlocal contributions only. However, due to the high symmetry of the $C_{\infty v}$ surface, they sort out chiral and achiral components: f_s, g_s, and h_p incorporate only chiral components and f_p, g_p, and h_s only achiral ones. Consequently, one can isolate a specific chiral component when choosing the right set of fundamental and harmonic polarizations. Nonlinear chiroptical effects are then expected to be stronger than linear ones, which appear only as a correction to the wave propagation. In conclusion, SHG is very sensitive to the molecular chirality because it is a three-wave mixing technique where a set of three electric field polarizations are adjustable to probe the three-dimensional conformational properties of molecules.

3.3. SHG Optical Activity. Three kinds of experiments are then relevant to probe the molecular chirality (see Figure 1). First, one can perform so-called "ORD-SHG" experiments similar to the optical rotation dispersion (ORD) experiments in linear optics: one analyzes the polarization of the SHG-reflected signal for a p-polarized fundamental laser beam. Any rotation of the former is a characteristic of the molecular chirality, because the SHG signal from an isotropic achiral surface is always p-polarized. The SHG rotation angle Φ scales as the ratio f_s/f_p where f_s vanishes unless the molecules are chiral. It is also possible to measure the relative phase of these parameters when considering their complex nature: $f_{s,p} = f'_{s,p} + if''_{s,p}$. For that purpose, one has to record the SHG signal for all angular positions (φ) of the analyzer and to fit the data with the following formula:[30]

$$I_{ORD}(2\omega) \propto (f'_p \cos\varphi + f'_s \sin\varphi)^2 + (f''_p \cos\varphi + f''_s \sin\varphi)^2 \quad (2)$$

In a second (respectively third) kind of experiment, one records the s- and p-polarization components of the SHG signal reflected by right or left circularly (respectively $\pm 45°$ linearly) polarized fundamental beam. Here also, any difference is characteristic of the molecular chirality. The circular difference (CD-SHG) may be considered as similar to the usual CD in linear optics although it is a coherent phenomenon and not an absorptive effect, whereas linear difference (LD-SHG) has no equivalent in linear optics. Here also, it is possible to measure the relative phase of the f, g, and h parameters when recording the SHG signal for all azimuthal positions θ_{wp} of the waveplate and fitting with the following formulas:[27,36]

$$I_{LD}(2\omega) \propto [(f' + g' + (f' - g')\cos 4\theta_{\lambda/2} + h' \sin 4\theta_{\lambda/2})^2 + (f'' + g'' + (f'' - g'')\cos 4\theta_{\lambda/2} + h'' \sin 4\theta_{\lambda/2})^2] \quad (3)$$

$$I_{CD}(2\omega) \propto [(f' - g' + 4f'' \cos 2\theta_{\lambda/4} - (f' - g')\cos 4\theta_{\lambda/4} + 2h'' \sin 2\theta_{\lambda/4} - h' \sin 4\theta_{\lambda/4})^2 + (f'' - g'' - 4f' \cos 2\theta_{\lambda/4} - (f'' - g'')\cos 4\theta_{\lambda/4} - 2h' \sin 2\theta_{\lambda/4} - h'' \sin 4\theta_{\lambda/4})^2] \quad (4)$$

The values of the LD-SHG and CD-SHG are deduced from these expressions applied to the relevant values of θ_{wp} ($\theta_{\lambda/2} = \pm 22.5°$ for LD, $\theta_{\lambda/4} = \pm 45°$ for CD), the differences in the corresponding SHG signals being normalized to their average values. Looking at eqs 2−4, one notes that ORD-SHG and LD-SHG appear as products of in-phase chiral and achiral parameters and CD-SHG as products of in-quadrature parameters. The latter is consistent with the definition of a circular polarization, which is a superposition of in-quadrature s- and p-polarization components. This phase sensitivity may be exploited to gain insight into the physical origin of the SHG optical activity. First, magnetic contributions are in-quadrature with electric ones, because they comprise a magnetic dipolar transition moment (or an electric quadrupolar one), which is dephased by 90° with the electric dipolar transition moment present in the usual local contribution.[42] In the particular case of SHG experiments performed off resonance, electric dipolar contributions may be considered as real and magnetic ones as imaginary in a good approximation. Second, the achiral parameters are usually dominated by electric dipolar contributions. One concludes from these considerations that ORD-SHG and LD-SHG experiments probe essentially the local chiral contributions and that these effects are expected to dominate when the molecular chirality arises from excitonic coupling. Conversely, CD-SHG is sensitive to nonlocal chiral contributions and is therefore characteristic of molecular chirality arising from one electron chirality.[31]

4. Experimental Results

4.1. Skin Multiphoton Microscopy. As we mentioned before, collagens I and IV can be found in different types of tissues. For example, in the skin, these collagens form different structures in distinct regions of the skin: collagen I is found in the dermis where it assembles in fibers that will give dermis its resistance to strain and traction, whereas collagen IV forms a network in the basement membrane. Figure 2a shows a combined 2PEF/SHG image of an unstained human skin histological cut. The 2PEF signal (red) is generated essentially in the upper layers of the epidermis by the keratin, in the lower layers by the cellular NADH, and in the skin dermis by the elastic fibers. The SHG signal (green) arises from the fibrillar collagen (essentially collagen I) found in the dermis. A dark line is visible between the epidermis and the dermis, which we attribute to the basement membrane region because its components (mainly laminin, entactin, perlecan, and collagen IV) are known not to exhibit fluorescence or SHG.[6,12] In particular, this 2PEF/SHG image clearly illustrates that fibrillar collagen I exhibits SHG, whereas collagen IV produces no signal under the same excitation conditions.

(42) Wagnière, G. H. *Linear and nonlinear optical properties of molecules*; VHCA: Basel, 1993.

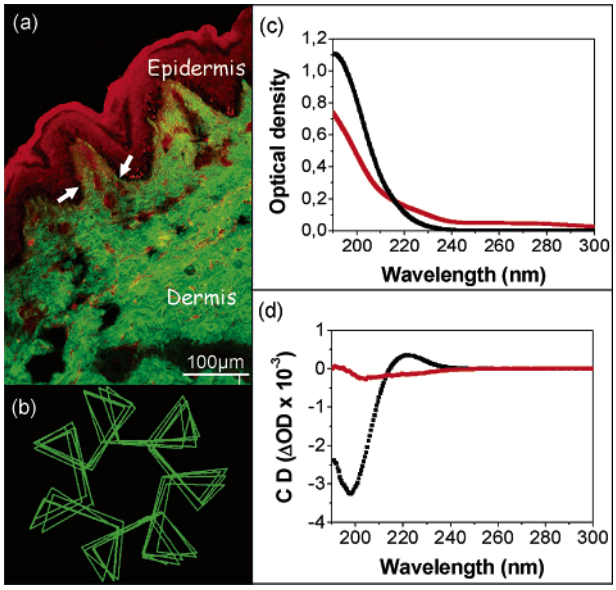

Figure 2. Multiphoton image, absorption, and CD spectra from collagens I and IV. (a) Combined 2PEF/SHG image of a thin unstained histological cut (human skin) acquired with a 20× (0.95 NA) water objective, and 4 mW power incident on the sample at 814 nm. 2PEF (in red) is detected in the backward channel (GG435 Schott, E700SP Chroma), and SHG (in green) is detected in the forward channel (interferential filter at 407 nm and 2 E700SP Chroma). (b) Axial view of the conformational structure of the triple-helical collagen-like peptide, $(Pro\text{-}Hyp\text{-}Gly)_4\text{-}Glu\text{-}Lys\text{-}Gly(Pro\text{-}Hyp\text{-}Gly)_5$ obtained from X-ray diffraction (Protein Data Bank), where the glycine residues are found inside the triple helix. (c) Optical density of 1.25 mg/mL solutions of (black) collagen I molecules and (red) collagen IV molecules, measured in a 100 μm-long fused silica (quartz) cell and normalized to the acetic acid solution. (d) CD spectra (variation in the optical density) of the same solutions in the same cells, with the same reference as in (c).

4.2. Sample Characterization. TEM Images. Figure 3b,c presents TEM images obtained with the collagen I in an acetic acid solution (b) and in a saline solution (c). The first image presents a homogeneous distribution, as further shown by the zoomed-in part in the inset. The second image presents fibrillar structures with a lateral size of 280 nm and a directional distribution attributed to the flow current during side drying of the sample on the TEM grid. It is characteristic of collagen fibrillar aggregation, as expected in a saline solution that enables the formation of collagen I fibrils in vitro. Conversely, there are no fibrils in the acetic acid solution, and the unstructured TEM image is consistent with a homogeneous distribution of triple helical molecules. In all our experiments, we always used the acetic acid solution of collagen I to avoid fibril assembly and to study collagen I molecules.

Absorption Spectra. Figure 2c presents the absorption spectra of the collagen I and IV solutions, and Figure 3a shows the absorption spectra of the collagen I and IV thin films. The film and solution spectra are very similar, which confirms that collagen molecules were successfully deposited on the fused silica substrate. All spectra present a band around 200 nm with a typical optical density of 0.15 (respectively 0.04) for the thin layer of collagen I molecules (respectively collagen IV molecules) and 0.8 (respectively 0.4) for the collagen I solution (respectively collagen IV solution) at 1.25 mg/mL concentration. These absorption spectra are typical for peptides composed of nonaromatic amino acids.

CD Spectra. Figure 2d presents the CD spectra of collagens I and IV molecules. They both exhibit a negative peak around

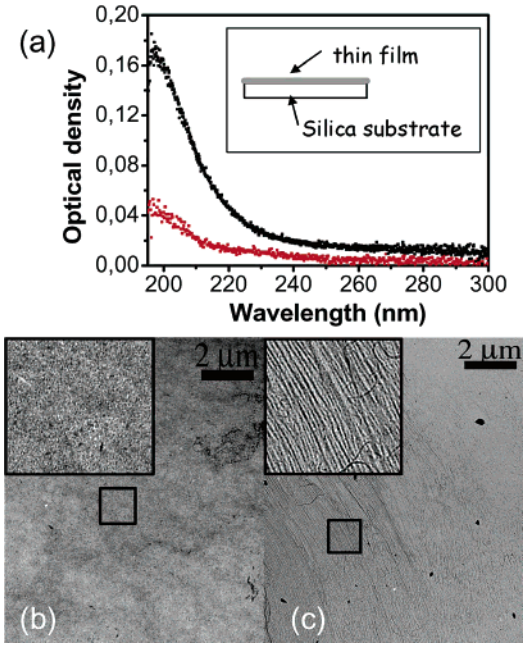

Figure 3. Thin film characterization. (a) Optical density of (black) thin layer of collagen I molecules and (red) collagen IV molecules, relative to the bare fused silica substrate. (b) TEM image of collagen I in acetic acid, showing a homogeneous distribution characteristic for collagen molecules. (c) TEM image of collagen I in a saline solution, showing a directional distribution characteristic for collagen fibrillar aggregation.

200 nm, in agreement with collagen I CD spectra already published in the literature.[43,44] This peak is characteristic of the so-called P_2 conformational structure and correlates with the particular structure of collagen I molecules, which are composed of three left-handed helices supercoiled in a right-handed triple helix. Figure 2b displays such a triple helical structure obtained with a collagen-like model peptide.

We note that the collagen IV CD is less intense than the collagen I CD: the extremum of the CD spectrum peaks at -0.25×10^{-3} for collagen IV and at -3.3×10^{-3} for collagen I, when measured in a 100 μm-long quartz (fused silica) cell, at a concentration of 1.25 mg/mL. This indicates that the triple helical structure is less present in collagen IV than in collagen I, in agreement with the flexible helical structure reported for that type of collagen whose triple helical domain presents short interruptions.

Fluorescence Spectra. We recorded the conventional fluorescence spectrum (1PEF) of the 1 mg/mL collagen I solution and observed no fluorescence upon excitation in the 210−300 nm range. We also observed no 2PEF signal when exciting in the 750−950 nm range at a power up to 6 GW/cm^3 at 800 nm. This indicates that the collagen fluorescence observed in tissues is not related to the collagen molecules and certainly originates in cross-links or particular structures implied in collagen fibers.[45]

4.3. SHG Optical Activity of Collagen Thin Films. We measured the polarization-resolved SHG signal reflected from these thin films of collagens I and IV upon excitation at 550 nm and 700−1000 nm. These experiments were performed in

(43) Bhatnagar, R. S.; Gough, C. A. In *Circular dichroism and the conformational analysis of biomolecules*; Fasman, G. D., Ed.; Plenum Press: New York, 1996; Chapter 6.
(44) Sreerama, N.; Woody, R. W. In *Numerical computer methods*; Brand, L., Johnson, M. L., Eds.; Elsevier: Amsterdam, 2004; Chapter 13.
(45) Richards-Kortum, R.; Sevick-Muraca, E. *Annu. Rev. Phys. Chem.* **1996**, *47*, 555−606.

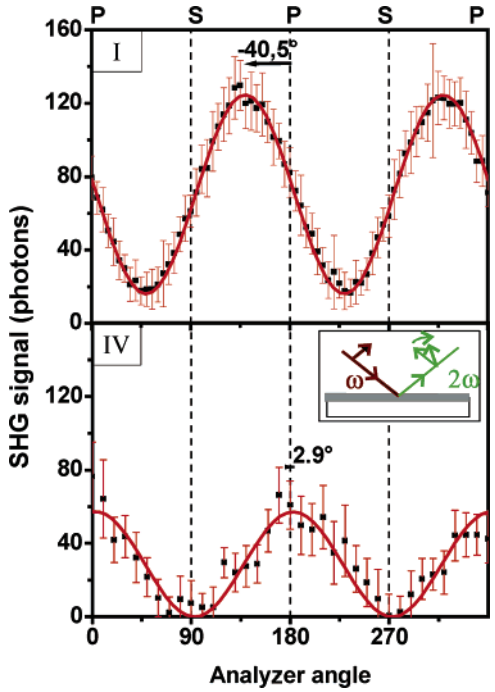

Figure 4. Reflected SHG signal versus the analyzer angle, for p-polarized incident laser beam ($\lambda = 800$ nm, $P = 400$ mW). Errors bars correspond to statistical errors when averaging 20 measurements (over 500 ms time integration), and the solid line corresponds to the fit with the formula (2). (Top) Collagen I molecules thin film. (Bottom) Collagen IV molecules thin film.

a nonresonant configuration, since the films did not exhibit any detectable one-photon or two-photon absorption in this wavelength range. This resulted in a reduced damage of the samples upon excitation at laser power up to 400 mW at 800 nm: we observed no significant fading of the signal after continuous illumination. The measurements were reproducible from one sample to another and for different angular orientations of the same sample. This indicates that our collagen films were isotropic and that the measured optical activity was related to the molecular chirality, rather than to orientational differences.

Surface SHG Experiments with Collagen I. First, we studied thin films of collagen I upon excitation at 800 nm. The samples presented a detectable SHG signal even in our conditions of nonresonant excitation. This signal was attributed to the collagen film since it was at least 10 times higher than the signal from the bare silica substrate.

Figure 4 presents the SHG signal as a function of the analyzer angle (see inset). The SHG polarization exhibits a clear rotation away from the p direction: fitting our results with a squared sinus, we obtained a rotation angle $\Phi = -40° \pm 5°$. The fitting accuracy was excellent, and the error bar was mainly due to the sample variability. Looking carefully at Figure 4, one notices that the SHG signal never drops to zero, which indicates that its f_p (p-polarized) and f_s (s-polarized) components do not possess the same phase. To determine the relative phase of f_p and f_s, we set $f_p = 1$ and used eq 2 to fit the SHG polarization dependency. We obtained $f_s = -0.66 + 0.60i$, which amounts to a phase difference of $-42°$. We use these relative values of f_s and f_p in the following as a quantitative relationship between the CD-SHG (or LD-SHG) experiments performed with a *p* and with an *s* analyzer (see first columns of Table 1).

The LD-SHG and CD-SHG results are displayed in Figure 5 for the *s* and *p* positions of the analyzer. LD measurements exhibit a 90° period and CD measurements exhibit a 180° period, consistent with the optical properties of half- or quarter-wave plates. The value of the LD is obtained as the difference in the signals for ±22.5° half-wave plate angles normalized to their average value: $LD_s = -76 \pm 2\%$ and $LD_p = -67 \pm 10\%$. The value of the CD is obtained as the difference in the signals for ±45° quarter-wave plate angles normalized to their average value: $CD_s = -16 \pm 6\%$ and $CD_p = -22 \pm 15\%$.

We further analyzed our data and used eqs 3 and 4 to extract the relative values of the *f*, *g*, and *h* parameters. Results are summarized in Table 1. The f_p value was set to 1 to provide a phase and amplitude reference. The particular choice of this phase reference was justified by the fact that, as a nonchiral parameter, f_p is dominated by local contributions, which are expected to be real in nonresonant experiments. The f_s value was obtained from the ORD experiments, and sets of *g* and *h* parameters were obtained for any of the s and p positions of the analyzer. During the fitting procedure, g_p and h_s were assumed to be real because they are achiral parameters like f_p. We note that:

(1) Equations 3 and 4 provide excellent fits to our experimental data, as evidenced by Figure 5 and the standard errors indicated in Table 1.

(2) Results obtained from the CD and LD curves are in reasonable agreement, considering that LD experiments have been shown to be less accurate than CD experiments for the determination of the *f*, *g*, and *h* parameters.[46]

(3) Detailed calculations show that f_s' and h_p' are both equal to the local chiral tensor components χ^{eee}_{xyz}, multiplied by similar geometrical factors (see Supporting Information). The values displayed in Table 1 have the same order of magnitude, although they do not show a quantitative agreement with this theoretical prediction.

(4) g_s shows a nonvanishing real part, although it is supposed to comprise only nonlocal parameters.

These remarks show that our results present a good qualitative, if not fully quantitative, agreement with the theoretical predictions. One may invoke the following reasons to explain the limits in the quantitative accuracy of our data analysis. First, error bars on the parameter values are larger than the statistical errors in the fitting procedure, because there are other error sources such as slight polarization misalignments. Second, the phase reference is somehow arbitrary since f_p does comprise some residual nonvanishing nonlocal components, and the assumption that h_s'', g_p'', and g_s' are zero is not perfectly valid. However, these assumptions aim at reducing the number of fitting parameters and giving an insight into the physical origin of the SHG signal. Within that formalism, we can conclude unambiguously from Table 1 that both local and nonlocal effects contribute to SHG chiroptical effects and that these effects are significant as shown by the modulus of the chiral parameters.

Finally, we measured the wavelength dependence of these chiroptical effects. For that purpose, we focused on the rotation angle measurements and limited our ORD-SHG experiments to a few wavelengths in the visible range. We obtained the following results: −34° at 874 nm excitation, −40° at 800 nm, −42° at 774 nm, and −60° at 550 nm excitation, with typical errors of ±5°. We note that all rotation angles have the same

(46) Maki, J. J.; Kauranen, M.; Verbiest, T.; Persoons, A. *Phys. Rev. B* **1997**, *55*, 5021−5026.

Table 1. Parameters and Standard Errors Obtained from the Fits of LD and CD Experiments Displayed in Figure 5[a]

experiment	f'	f''	g'	g''	h'	h''
s-LD	-0.66^b	0.6^b	-0.58 ± 0.03^b	0.59 ± 0.06^b	4.60 ± 0.14^c	0^c
s-CD	-0.66^b	0.6^b	-0.74 ± 0.10^b	0.48 ± 0.03^b	4.43 ± 0.15^c	0^c
p-LD	1^c	0^c	1.09 ± 0.01^c	0^c	-0.37 ± 0.01^b	0.22 ± 0.18^b
p-CD	1^c	0^c	1.77 ± 0.05^c	0^c	-0.39 ± 0.02^b	0.15 ± 0.04^b

[a] f_p is set to 1 to provide a phase and amplitude reference, and the value of f_s relative to that of f_p is given by the fit of ORD experiment displayed in Figure 4. [b] Chiral parameters. [c] Achiral parameters.

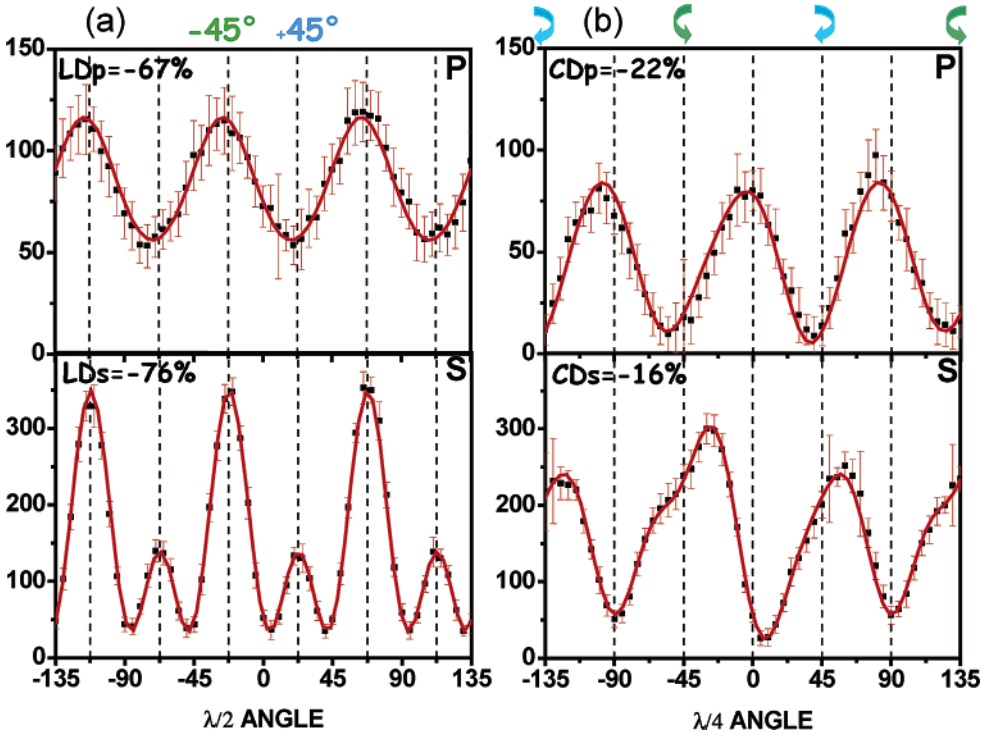

Figure 5. p-Polarized (top) and s-polarized (bottom) component of the SHG signal reflected from collagen I molecules thin film, versus the azimuthal angle of the (a) $\lambda/2$ and (b) $\lambda/4$ plates ($\lambda = 800$ nm, $P = 400$ mW). Errors bars correspond to statistical errors when averaging 20 measurements (over 500 ms time integration), and the solid line corresponds to the fit with eq 3 and the parameters indicated in Table 1.

sign and order of magnitude, with a steady increase when decreasing the excitation wavelength.

Surface SHG Experiments with Collagen IV. We then performed the same experiments at 800 nm excitation with the collagen IV films. The samples exhibited a small but detectable SHG signal. The order of magnitude of this signal was typically half the one of collagen I, as shown on Figure 4. When looking at the p-polarized component, one sees that the achiral part of the signal (60 photons/500 ms) has almost the same magnitude as in collagen I (80 photons/500 ms). Remarkably, we observed no rotation of the SHG signal reflected from collagen IV films. Figure 4 shows that it is perfectly p-polarized as for nonchiral surfaces. Similar results were obtained with CD and LD experiments (data not shown): the curves we obtained were symmetrical and showed no difference for ±45° linear and right/left circular polarization of the incident laser beam.

5. Discussion

Our experiments aimed at measuring chiroptical effects from collagen molecules and at comparing the optical properties of fibril-forming collagen I and nonfibrillar collagen IV. Our absorption, fluorescence, and TEM data confirm that we recorded signals from collagen molecules, with no formation of fibrils. Conventional CD spectra and SHG optical activity measurements showed consistent results: fibril-forming collagen I exhibits linear and nonlinear chiroptical effects, whereas nonfibrillar collagen IV presents a smaller linear optical activity and no SHG optical activity. We pointed out in the Experimental Section that collagen IV exhibits much smaller CD than collagen I, and we inferred that the P_2 conformational structure is less present in collagen IV, in agreement with the numerous short interruptions in the triple helical domain reported for this type of collagen. We conclude from the similarity between CD and SHG measurements that the absence of any chiroptical effects in the SHG from collagen IV is also due to the numerous interruptions in its helical domain, which likely decreases the overall chirality of the molecule.

Let us now consider the SHG optical activity from collagen I. When looking at the dependence on the excitation wavelength, we observed that the magnitude of the SHG rotation angle increases significantly when exciting closer to the absorption peak at 200 nm. This result is consistent with model calculations developed for excitonic coupling[28] and more generally with the Kleinman symmetry. The latter states that, away from any resonance, all the susceptibility tensor components are equal in the electric dipolar approximation. In particular, $\chi^{eee}_{xyz} = \chi^{eee}_{zyx}$, and as the opposite relationship applies for chiral molecules, this component vanishes, as well as all chiral components in

the electric dipolar susceptibility tensor. Consequently, it is not possible to observe any chiroptical effects when applying the Kleinman symmetry. This approximation is strictly valid in the electric dipolar approximation, away from any one- or two-photon resonance, and chiroptical effects are expected to increase when approaching resonances. This is qualitatively consistent with our experimental observations, although the chiroptical effects we measured upon excitation around 800 nm are unexpectedly large, considering that the absorption peak around 200 nm is still away from the second harmonic wavelength at 400 nm. This quantitative discrepancy can be explained by the existence of contributions other than the electric dipolar ones to the SHG optical activity. The latter assumption arises from the phase measurements of the *f*, *g*, and *h* parameters, bearing in mind the 90° phase difference between electric and magnetic contributions: if we consider that the achiral component f_p is dominated by electric contributions, Table 1 indicates that the chiral component f_s comprises electric ($f_s' = -0.66$) and magnetic ($f_s'' = 0.6$) contributions together, typically with the same order of magnitude. This result can also be deduced qualitatively from the combination of ORD-SHG and LD-SHG measurements, which are mainly sensitive to electric contributions, and CD-SHG measurements, which are mainly sensitive to magnetic contributions. Both types of polarization-resolved SHG experiments exhibit large optical activity in nonresonant conditions, which indicates a mixing of electric and magnetic contributions. Consequently, the physical origin of collagen optical activity arises from mechanisms more complex than excitonic coupling or one-electron chirality and involves both mechanisms. However, it is not possible to deduce from our data which electric and magnetic dipoles couple on which transitions to exhibit such a large SHG optical activity. This limitation looks similar to the difficulties encountered to model the collagen CD: present theoretical methods do not adequately reproduce the CD of collagen, although they are able to reproduce the CD of other protein conformations.[43,44] It indicates the complexity of the physical origin of collagen linear and nonlinear optical activity.

Our thorough analysis of the collagen I SHG optical activity provides a quantitative order of magnitude for the chiral contributions. Let us focus again on the ORD-SHG experiments and compare the magnitude of the f_s and f_p parameters: one obtains $(|f_s|^2/|f_p|^2) = 0.8$ at 800-nm excitation. Considering a p-polarized excitation, the total SHG intensity comprises a chiral component $I_{chiral} \propto |f_s|^2$and an achiral component $I_{achiral} \propto |f_p|^2$:

$$I(2\omega) = I_{chiral} + I_{achiral} \propto |f_s|^2 + |f_p|^2 \qquad (5)$$

with no analyzer. Because $|f_s|^2 \approx |f_p|^2$, the chiral contribution has typically the same order of magnitude as the achiral one. Consequently, chirality enhances collagen I SHG by a factor 2. This factor may vary to some extent when changing the excitation wavelength or the incident polarization, but still provides a quantitative order of magnitude for the chiral enhancement in surface SHG.

The generalization to SHG microscopy in collagen tissue needs to be carefully analyzed. In our surface experiments, the achiral component of the susceptibility arises from the averaging of achiral components of molecular hyperpolarizabilities over a thin two-dimensional layer of collagen molecules. This isotropic film is at least partially polarized (that is, molecules have a definite orientation relative to the substrate), otherwise there would be no achiral SHG. Looking at the structure of collagen molecules in acetic acid, the C-terminal carboxylic acids are hydrophobic and the N-terminal NH_3^+ functions are hydrophilic. We then expect the collagen molecules to be polarized on the hydrophilic silica substrate with the ammonium down on the substrate. However, the degree of polarity and the average angle of the collagen triple helix to the surface normal are not quantitatively determined. Consequently, our surface experiments do not provide a quantitative value of the achiral susceptibility, which may be different in bulk collagen. In the latter case, the collagen molecules are polarized in nanofibrils, although this polarity may be partially lost at the micrometer scale[10,47] so that the achiral component of the susceptibility may be stronger than in surface experiments. To summarize, whereas the chiral contributions are not sensitive to polarity, the achiral contributions vary with the polarity and may be underestimated in surface experiments compared to bulk SHG. However, our surface SHG data still provide a qualitative order of magnitude for the chiral contributions to collagen SHG and show that the chiral enhancement of collagen SHG is less than a factor 2. Consequently, the collagen chirality is not responsible for the large collagen SHG signals observed in connective tissue microscopy. As previously suggested, the high collagen I SHG efficiency is presumably due to the high density and crystalline order in collagen fibrils.

The importance of the collagen fibrils structure is further illustrated when comparing collagens I and IV. Our experimental data show that the surface SHG signals from collagen I and IV thin films have typically the same order of magnitude, although these two types of collagen exhibit strikingly different behavior in connective tissue "bulk" SHG microscopy. The skin multiphoton image displayed in Figure 1 illustrates that no SHG signal is detected from collagen IV in the basement membrane, whereas a large signal arises from collagen I fibers in the same conditions of excitation. One must bear in mind that SHG vanishes in bulk isotropic media (even in isotropic assemblies of chiral molecules, where only sum frequency generation is allowed[37]). Therefore, our surface and bulk SHG data show that the macroscopic organization of collagen IV molecules in the basement membrane is nearly isotropic, in agreement with the reported architecture of basement membranes.[16] To conclude, collagen IV molecules form networks with no preferential directional ordering of the helical domains, so that bulk SHG vanishes, even though the molecular hyperpolarizability is nonzero according to surface SHG experiments.

6. Conclusion

In this article, we presented a comprehensive study of the chiroptical properties of fibril-forming collagen I and nonfibrillar collagen IV, including polarization-resolved surface SHG experiments and conventional CD spectroscopy. We observed little CD and no SHG optical activity from collagen IV, presumably due to the numerous interruptions in its helical domain, which decreases the overall chirality of the molecule. Collagen I exhibits a large optical activity in SHG and CD experiments, which can be attributed to one-electron and excitonic coupling contributions. However, we estimated that

(47) Holmes, D. F.; Graham, H. K.; Trotter, J. A.; Kadler, K. E. *Micron* **2001**, *32*, 273−285.

the resulting chiral enhancement in collagen SHG microscopy is less than a factor 2. Consequently, the large collagen I SHG efficiency is dominated by coherent effects due to the high density and crystalline order in collagen fibrils. Conversely, we attributed the absence of any SHG from collagen IV in basement membranes to the lack of alignment of the helical domains: our surface SHG experiments showed that the molecular hyperpolarizability has typically the same order of magnitude as for collagen I, and the susceptibility vanishes presumably due to isotropic averaging.

The results of our thin film experiments may be generalized to other collagen types, assuming that most collagen molecules present similar second-order hyperpolarizabilities. Consequently, it should be noted that, unlike immunohistochemistry, SHG microscopy is sensitive to the organization of collagen molecules in the tissue, rather than to the collagen type. To conclude, SHG microscopy probes collagen macromolecular structure at the micrometer scale, which makes it a powerful technique to study collagen organization in biological tissues. Several applications can be envisioned, from the study of collagen fibrillogenesis in normal or injured tissue, to the study of its remodeling during wound healing and revascularization or the characterization of the pathological organizations of connective tissue in tumors.[48]

Acknowledgment. We thank François Hache, Yann Bretonnière, and Emmanuel Beaurepaire for fruitful discussions, Gaston Godeau for providing us with the skin histological cuts, and Gervaise Mosser for TEM characterization.

Supporting Information Available: Full mathematical expressions of the *f*, *g*, and *h* parameters as a function of the tensor components of the χ^{eee}, χ^{eem} and χ^{mee} second-order susceptibilities. This material is available free of charge via the Internet at http://pubs.acs.org.

JA0520969

(48) Brown, E.; McKee, T.; diTomaso, E.; Pluen, A.; Seed, B.; Boucher, Y.; Jain, R. K. *Nat. Med.* **2003**, *9*, 796−800.